The American Journal of Human Genetics, Volume *108*

Supplemental information

TNPO2 variants associate with human developmental delays, neurologic deficits, and dysmorphic features and alter *TNPO2* activity in *Drosophila*

Lindsey D. Goodman, Heidi Cope, Zelha Nil, Thomas A. Ravenscroft, Wu-Lin Charng, Shenzhao Lu, An-Chi Tien, Rolph Pfundt, David A. Koolen, Charlotte A. Haaxma, Hermine E. Veenstra-Knol, Jolien S. Klein Wassink-Ruiter, Marijke R. Wevers, Melissa Jones, Laurence E. Walsh, Victoria H. Klee, Miel Theunis, Eric Legius, Dora Steel, Katy E.S. Barwick, Manju A. Kurian, Shekeeb S. Mohammad, Russell C. Dale, Paulien A. Terhal, Ellen van Binsbergen, Brian Kirmse, Bethany Robinette, Benjamin Cogné, Bertrand Isidor, Theresa A. Grebe, Peggy Kulch, Bryan E. Hainline, Katherine Sapp, Eva Morava, Eric W. Klee, Erica L. Macke, Pamela Trapane, Christopher Spencer, Yue Si, Amber Begtrup, Matthew J. Moulton, Debdeep Dutta, Oguz Kanca, Undiagnosed Diseases Network, Michael F. Wangler, Shinya Yamamoto, Hugo J. Bellen, and Queenie K.-G. Tan

Supplemental Note S1: Case reports.

Proband 5 carries three *de novo,* heterozygous VUS in addition to the reported variant in *TNPO2*. First, is a frameshift variant in *SET binding protein 1* (*SETBP1*; NM_015559): c.4565delinsGGC (p.Leu1522Argfs*59). *SETBP1* encodes a DNA-binding protein that is involved in chromatin dynamics and gene expression. *SETBP1* is a highly constrained gene – misZ=1.10 (o/e=0.90), pLI=1.00 (o/e=0.02) – and has been associated with mental retardation, autosomal dominant 29 (MIM: 616078) and Schinzel-Giedion midface retraction syndrome; autosomal dominant (MIM: 269150). Importantly, this variant is considerably further down in the gene than known pathogenic variants[1], falling within the last exon in the canonical transcript about 70 amino acids from the end. Further, the proband has no features suggestive of Schinzel-Giedion syndrome[2]. A second, *de novo*, heterozygous SNV is detected in *Cut-like Homeobox 2* (*CUX2*; NM_015267):c.3758A>C (p.His1253Pro). *CUX2* is highly constrained – misZ=3.18 (o/e=0.70), pLI=1.00 (o/e=0.09) – and has been associated with developmental and epileptic encephalopathy 67 (MIM: 618141; autosomal dominant). *CUX2* encodes a transcription factor involved in neuron morphogenesis and synaptic plasticity. Variants in the gene have recently been associated with rare cases involving intellectual disability, seizures and ASD[3]. However, the variant in our proband is not predicted to be pathogenic by SIFT, PolyPhen and Align GVGD and is associated with a CADD score of 17.1. As this individual's *TNPO2* variant causes a deletion at an amino acid conserved in mammals, the *TNPO2* variant is the primary candidate to explain the individual's features, and the mosacism may explain the proband's relatively mild features. The last VUS detected in our proband is a 12q13.13 duplication that was determined to unlikely be clinically relevant. Overall, the proband's variant in *TNPO2* was the most likely candidate for further study.

Proband 6 carries a *de novo,* heterozygous deletion/insertion in *Rabankyrin-5* (*ANKFY1;* NM_001257999.2): c.3263delinsGCT (p.Thr1088Serfs*9) in addition to the reported variant in *TNPO2*. *ANKFY1* is a moderately constrained gene – misZ= 2.46 (o/e=0.74), pLI= 0.96 (o/e=0.19) – that has not been associated with Mendelian disease. *ANKFY1* encodes a cytoplasmic protein that is predicted to be involved in vesicle or protein transport. Given the relatively lower gene constraint compared to *TNPO2*, this variant is not the primary candidate for further investigation to explain the proband's features.

Proband 8 carries a *de novo,* heterozygous SNV in *Armadillo repeat containing 9* (*ARMC9;* NM_025139.3):c.988G>A (p.Asp330Asn) in addition to a TNPO2 variant. The ARMC9 variant has a CADD score of 24 and is not found in gnomAD. This gene is lowly constrained – misZ=0.85 (o/e=0.88), pLI=0.00 (o/e=0.78) – while variants in *ARMC9* have been associated with the autosomal recessive Joubert syndrome 30 (MIM: 617622). Given the low constraint of this gene and the presence of only one variant in an autosomal recessive disorder, it is not the primary candidate to explain this individual's symptoms.

Proband 10 carries three *de novo,* heterozygous CNVs (two micro-insertions and one micro-deletion) and three *de novo,* heterozygous SNVs in genes with lower constraint than *TNPO2* in addition to the reported *TNPO2* variant. The most notable of these is a 522 Kb gain at 1q21.1 (1:g.145,287,319-145,809,279)x3). Genes impacted by these VUS are not associated with disease and do not explain the individual's symptoms. Overall, these VUS were not considered the explanation for the proband's features.

Proband 14 carries a *de novo,* heterozygous SNV in *Phosphodiesterase-4D* (*PDE4D;* NM_001104631.1): c.709C>T (p.Arg237*) in addition to the reported variant in *TNPO2*. The *PDE4D* variant corresponds to a CADD score of 37.0 and is not found in gnomAD. The gene is highly constrained – misZ=3.75 (o/e=0.47), pLI= 1.00, (o/e=0.08). *PDE4D* encodes a cAMP phosphodiesterase that mediates cAMP degradation and plays a critical roles in synaptic

plasticity and development. Variants within *PDE4D* are associated with acrodysostosis 2 (ACRDYS2 [MIM: 614613]) and truncating variants are associated with an intellectual disability (ID) syndrome[4]. The features of this proband is thought to be consistent with *PED4D*-associated ID syndrome, but the *de novo TNPO2* variant likely plays an additive role in his disease presentation.

Proband 15 carries a *de novo,* heterozygous SNV in *α-Internexin* (*INA*; NM_032727.4): c.1127T>C (p.Leu376Pro) that is mosaic (20% of reads) in addition to the reported variant in *TNPO2*. This *INA* variant has a CADD score of 30.0, is not found in gnomAD, and has not been associated with a Mendelian disease. Because INA is a lowly constrained gene – misZ= 2.13 (o/e=0.63), pLI= 0.00 (o/e=0.88) – and this variant is mosaic, it is not the primary candidate to explain the proband's symptoms. *INA* encodes a Class-IV neuronal intermediate filament and is not currently known to be associated with human disease.

Supplemental Note S2: UDN consortia co-investigators

The Undiagnosed Diseases Network (UDN) co-investigators are Maria T. Acosta, Margaret Adam, David R. Adams, Pankaj B. Agrawal, Mercedes E. Alejandro, Justin Alvey, Laura Amendola, Ashley Andrews, Euan A. Ashley, Mahshid S. Azamian, Carlos A. Bacino, Guney Bademci, Eva Baker, Ashok Balasubramanyam, Dustin Baldridge, Jim Bale, Michael Bamshad, Deborah Barbouth, Pinar Bayrak-Toydemir, Anita Beck, Alan H. Beggs, Edward Behrens, Gill Bejerano, Jimmy Bennet, Beverly Berg-Rood, Jonathan A. Bernstein, Gerard T. Berry, Anna Bican, Stephanie Bivona, Elizabeth Blue, John Bohnsack, Carsten Bonnenmann, Devon Bonner, Lorenzo Botto, Brenna Boyd, Lauren C. Briere, Elly Brokamp, Gabrielle Brown, Elizabeth A. Burke, Lindsay C. Burrage, Manish J. Butte, Peter Byers, William E. Byrd, John Carey, Olveen Carrasquillo, Ta Chen Peter Chang, Sirisak Chanprasert, Hsiao-Tuan Chao, Gary D. Clark, Terra R. Coakley, Laurel A. Cobban, Joy D. Cogan, Matthew Coggins, F. Sessions Cole, Heather A. Colley, Cynthia M. Cooper, Heidi Cope, William J. Craigen, Andrew B. Crouse, Michael Cunningham, Precilla D'Souza, Hongzheng Dai, Surendra Dasari, Joie Davis, Jyoti G. Dayal, Matthew Deardorff, Esteban C. Dell'Angelica, Shweta U. Dhar, Katrina Dipple, Daniel Doherty, Naghmeh Dorrani, Argenia L. Doss, Emilie D. Douine, David D. Draper, Laura Duncan, Dawn Earl, David J. Eckstein, Lisa T. Emrick, Christine M. Eng, Cecilia Esteves, Marni Falk, Liliana Fernandez, Carlos Ferreira, Elizabeth L. Fieg, Laurie C. Findley, Paul G. Fisher, Brent L. Fogel, Irman Forghani, William A. Gahl, Ian Glass, Bernadette Gochuico, Rena A. Godfrey, Katie Golden-Grant, Alica M. Goldman, Madison P. Goldrich, David B. Goldstein, Alana Grajewski, Catherine A. Groden, Irma Gutierrez, Sihoun Hahn, Rizwan Hamid, Neil A. Hanchard, Athena Hantzaridis, Kelly Hassey, Nichole Hayes, Frances High, Anne Hing, Fuki M. Hisama, Ingrid A. Holm, Jason Hom, Martha Horike-Pyne, Alden Huang, Yong Huang, Laryssa Huryn, Rosario Isasi, Fariha Jamal, Gail P. Jarvik, Jeffrey Jarvik, Suman Jayadev, Lefkothea Karaviti, Jennifer Kennedy, Dana Kiley, Shilpa N. Kobren, Isaac S. Kohane, Jennefer N. Kohler, Deborah Krakow, Donna M. Krasnewich, Elijah Kravets, Susan Korrick, Mary Koziura, Joel B. Krier, Seema R. Lalani, Byron Lam, Christina Lam, Grace L. LaMoure, Brendan C. Lanpher, Ian R. Lanza, Lea Latham, Kimberly LeBlanc, Brendan H. Lee, Hane Lee, Roy Levitt, Richard A. Lewis, Sharyn A. Lincoln, Pengfei Liu, Xue Zhong Liu, Nicola Longo, Sandra K. Loo, Joseph Loscalzo, Richard L. Maas, John MacDowall, Ellen F. Macnamara, Calum A. MacRae, Valerie V. Maduro, Bryan C. Mak, May Christine V. Malicdan, Laura A. Mamounas, Teri A. Manolio, Rong Mao, Kenneth Maravilla, Thomas C. Markello, Ronit Marom, Gabor Marth, Beth A. Martin, Martin G. Martin, Julian A. Martínez-Agosto, Shruti Marwaha, Jacob McCauley, Allyn McConkie-Rosell, Alexa T. McCray, Elisabeth McGee, Heather Mefford, J. Lawrence Merritt, Matthew Might, Ghayda Mirzaa, Eva Morava, Paolo M. Moretti, Deborah Mosbrook-Davis, John J. Mulvihill, David R. Murdock, Anna Nagy, Mariko Nakano-Okuno, Avi Nath, Stan F. Nelson, John H. Newman, Sarah K. Nicholas, Deborah Nickerson, Shirley Nieves-Rodriguez, Donna Novacic, Devin Oglesbee, James P. Orengo, Laura Pace, Stephen Pak, J. Carl Pallais, Christina GS. Palmer, Jeanette C. Papp, Neil H. Parker, John A. Phillips III, Jennifer E. Posey, Lorraine Potocki, Bradley Power, Barbara N. Pusey, Aaron Quinlan, Wendy Raskind, Archana N. Raja, Deepak A. Rao, Genecee Renteria, Chloe M. Reuter, Lynette Rives, Amy K. Robertson, Lance H. Rodan, Jill A. Rosenfeld, Natalie Rosenwasser, Francis Rossignol, Maura Ruzhnikov, Ralph Sacco, Jacinda B. Sampson, Susan L. Samson, Mario Saporta, C. Ron Scott, Judy Schaechter, Timothy Schedl, Kelly Schoch, Daryl A. Scott, Vandana Shashi, Jimann Shin, Rebecca Signer, Edwin K. Silverman, Janet S. Sinsheimer, Kathy Sisco, Edward C. Smith, Kevin S. Smith, Emily Solem, Lilianna Solnica-Krezel, Ben Solomon, Rebecca C. Spillmann, Joan M. Stoler, Jennifer A. Sullivan, Kathleen Sullivan, Angela Sun, Shirley Sutton, David A. Sweetser, Virginia Sybert, Holly K. Tabor, Amelia L. M. Tan, Queenie K.-G.Tan, Mustafa Tekin, Fred Telischi, Willa Thorson, Audrey Thurm, Cynthia J. Tifft, Camilo Toro, Alyssa A. Tran, Brianna M. Tucker, Tiina K. Urv, Adeline Vanderver, Matt Velinder, Dave Viskochil, Tiphanie P. Vogel, Colleen E. Wahl,

Stephanie Wallace, Nicole M. Walley, Chris A. Walsh, Melissa Walker, Jennifer Wambach, Jijun Wan, Lee-kai Wang, Michael F. Wangler, Patricia A. Ward, Daniel Wegner, Mark Wener, Tara Wenger, Katherine Wesseling Perry, Monte Westerfield, Matthew T. Wheeler, Jordan Whitlock, Lynne A. Wolfe, Jeremy D. Woods, Shinya Yamamoto, John Yang, Muhammad Yousef, Diane B. Zastrow, Wadih Zein, Chunli Zhao, Stephan Zuchner.

A ***dTnpo* Knockdown**

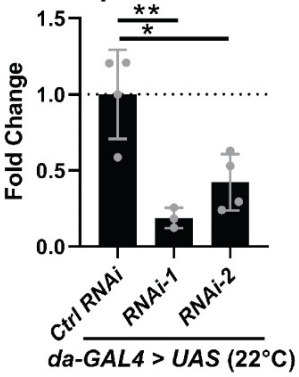

B **Stage of death with RNAi**

25°C	*da-GAL4*
dTnpo RNAi-1	L2*
dTnpo RNAi-2	L3*

* in rare cases escaper puparia are observed

C ***nub-GAL4* (25°C), lethal with RNAi-1**

D ***ey-GAL4* (~22°C), lethal with RNAi-1**

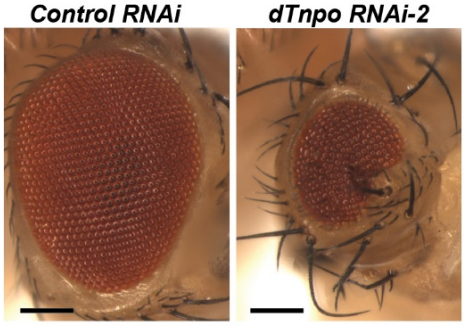

E ***GMR-GAL4* (25°C)**

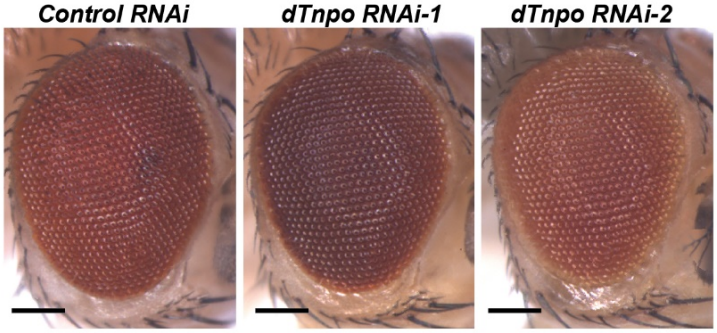

F **Summary of effects when *dTnpo* is downregulated in specific tissues using *GAL4 > UAS-RNAi***

GAL4 Driver	Primary Tissue(s)	Stage	*UAS-dTnpo RNAi-1*	*UAS-dTnpo RNAi-2*
Ubiquitous				
daughterless (da)-GAL4	ubiquitous	embryonic-adult	Larval lethal (18-29°C): L2 at 25°C	Larval lethal (25°C); pupal lethal (22°C)
daughterless (da)-GAL4[GS]	ubiquitous	adult (drug-induced)	reduced lifespan (29°C)	n/a
Nervous system				
inscuteable (insc)-GAL4	neuroblasts	embryonic	no obvious phenotypes (25°C)	no obvious phenotypes (25°C)
elav-GAL4	neurons	embryonic-adult	Lethal: larval at 29°C, pupal at ≤25°C	no obvious phenotype (≤29°C, 10d)
elav-GAL4[GS]	neurons	adult (drug-induced)	reduced lifespan (29°C)	n/a
Optic system				
eyeless (ey)-GAL4	developing eye	embryonic-adult	Larval lethal (25°C); pupal lethal (≤22°C)	morphological defects (18-29°C)*,#
GMR-GAL4 (Glass)	developing retina, photorecepter cells	3rd instar-adult	no external eye phenotype (25°C)	no external eye phenotype (25°C)
Rh1-GAL4 (NinaE)	photoreceptor neurons	adult	ERG defects at 7d (29°C)	mild ERG defects at 22d (29°C)
Thorax				
nubbin (nub)-GAL4	ventral thoracic disc, wing disc, haltere disc	embryonic-adult	Lethal: larval at 25°C, pupal at 22°C**	severe wing and haltere phenotypes (22-25°C)*
wingless (wg)-GAL4	ventral thoracic disc, wing disc, haltere disc	embryonic-adult	Larval lethal (22-25°C)	Lethal: larval at 25°C, pupal at 22°C

* pupal lethal at higher expression with escapers

expression-dependent defects with more severe phenotypes at higher temperatures

** likely lethal at 18°C but CyO phenotype on balancer was suppressed so difficult to define flies with desired genotype

Figure S1: *dTnpo* RNAi cause tissue-specific phenotypes, including disruptions in animal, wing, and eye development. (**A**) *UAS-dTnpo RNAi* were ubiquitously expressed in L2-L3 larvae using *da-GAL4*. qPCR was used to define *dTnpo* mRNA levels. Animals were raised at room-temperature (~22°C). Statistics: 1-way ANOVAs with Dunnett's multiple comparisons test. P-value **<0.01. Error bars denote SD. Each dot represents the mean from replicate wells per sample. The mean from 3-4 individual samples is shown. **(B)** Ubiquitous expression of *dTnpo* RNAi using *da-GAL4* at 25°C causes lethality in larval stages. **(C)** Expression of *dTnpo* RNAi using *nub-GAL4* causes lethality with RNAi-1 and robust morphologic defects with RNAi-2. **(D)** Expression of *dTnpo* RNAi using *ey-GAL4* causes lethality with RNAi-1 and robust morphologic defects with RNAi-2, including a small eye and a rough eye phenotype. **(E)** Expression of *dTnpo* RNAi-1 in later stages of eye development using *GMR-GAL4* does not dramatically alter the external eye. *dTnpo* RNAi-2 expression causes a mild reduction in eye size. **(F)** Table summarizing the impacts of expressing *dTnpo*-targeting RNAi in different fly tissues and at different temperatures under control of the *GAL4/UAS* system. Red indicates conditions where the *dTnpo* RNAi disrupts expected "control" phenotypes. RNAi lines: "Control RNAi" is *UAS-Luciferase RNAi* (TRiP.JF01355), *UAS-dTnpo RNAi-1* is TRiP.HMJ23009, and *UAS-dTnpo RNAi-2* is KK108990.

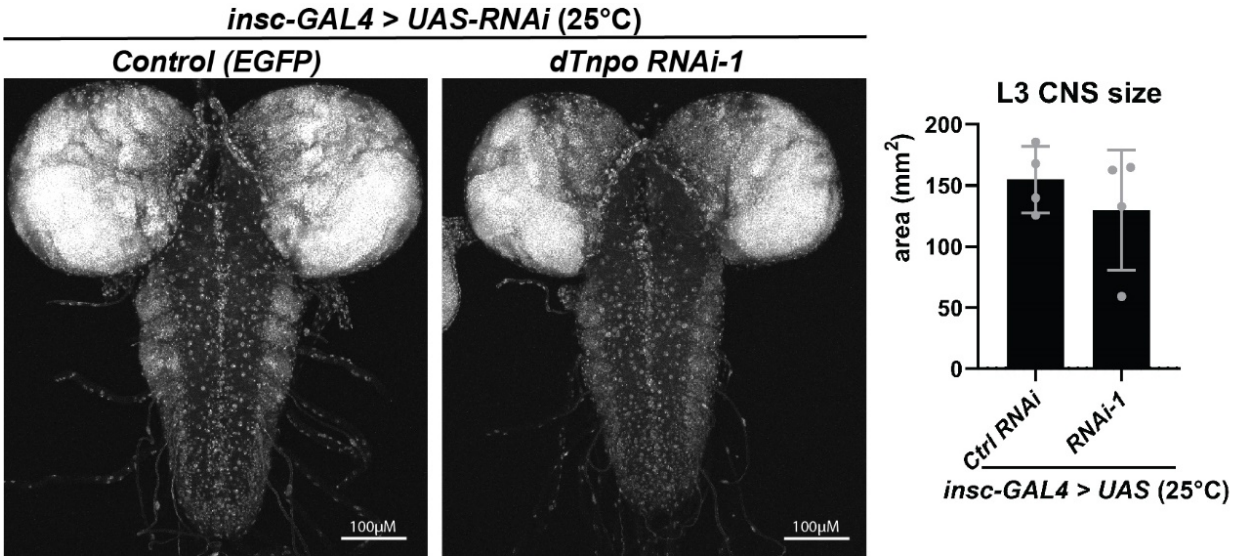

Figure S2: *dTnpo* RNAi expression in neuroblasts does not significantly reduce L3 CNS size. Expression of *dTnpo* RNAi in neuroblasts of the developing brain using *insc-GAL4* did not significantly alter the size of L3 CNS when compared to animals expressing a control RNAi targeting EGFP. Animals were raised at 25°C and CNS were dissected from wandering L3 animals right before pupariation as previously described[5]. Brains were counterstained with DAPI for imaging. The tissue area was measured from the 2-dimensional, Z-stacked images. Statistics: student t-test. Error bars denote SD. Each dot represents the area of the CNS from one animal.

A **Stage of death for *dTnpo* mutant flies expressing hTNPO2**

25°C	*dTnpo CRIMIC* (T2A-GAL4) > UAS						
	UAS Control	*hTNPO2*					
		WT	*p.Gln28Arg*	*p.Asp156Asn*	*p.Trp370Cys*	*p.Ala546Val*	*p.Trp727Cys*
dTnpo CRiMIC/ dTnpo[Gly736Asp]	L3*	L2*	L2*	L2*	L3*	L3*	L2*

*in rare cases puparia could be observed

B **Observed Mendelian ratios**

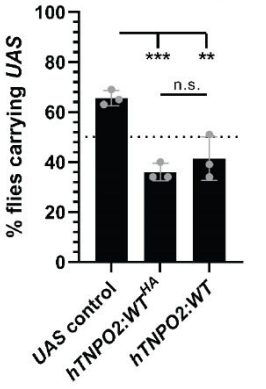

da-GAL4 x *UAS/Balancer* (25°C)

C **Summary of effects when *UAS-hTNPO2* lines are expressed in different tissues**

GAL4 Driver	Primary Tissue(s)	Stage	*UAS-hTNPO2*						
			WT ^{HA}	*p.Gln28Arg*	*p.Asp156Asn*	*p.Trp370Arg*	*p.Trp370Cys*	*p.Ala546Val*	*p.Trp727Cys*
Summary of variant impact versus wild-type hTNPO2									
Variant toxicity versus hTNPO2:WT^{HA}				↑↑↑	↑↑↑	↓↓	↓↓	↓	↓↓↑
Location in hTNPO2 protein				**RAN binding**		**Acidic loop**		**Cargo binding**	
Ubiquitous expression									
daughterless (da)-GAL4	ubiquitous	embryonic-adult	48% lethal at 25°C (p=0.001) vs UAS control; no significant lethality at 22°C	97% lethal at 25°C (p<0.0001) vs UAS control; 91% lethal at 22°C* (p<0.0001) vs UAS control	75% lethal at 25°C (p<0.0001) vs UAS control; 39% lethal 22°C* (p=0.04) vs UAS control	31% lethal at 25°C (p=0.01) vs UAS control; no significant lethality at 22°C	31% lethal at 25°C (p=0.01) vs UAS control; no significant lethality at 22°C	50% lethal at 25°C (p<0.0001) vs UAS control; no significant lethality at 22°C	no significant lethality at ≥22°C vs UAS control
Expression in the developing eye									
eyeless (ey)-GAL4	early eye development	embryonic-adult	phenotype at 29°C; rare phenotypes at ≤25°C	phenotypes at 29°C common; rare phenotypes at ≤25°C	phenotypes at 29°C common; rare phenotypes at ≤25°C	rare phenotypes ≥22°C	rare phenotypes ≥22°C	phenotypes at 29°C common; rare phenotypes at ≤25°C	some phenotypes at 29°C; rare phenotypes at ≤25°C
GMR-GAL4 (Glass)	late eye development, retina, some L3 brain expression	3rd instar-adult	mild rough eye phenotype 25°C; no phenotype at 22°C	rough eye phenotype ≥22°C	lethal at 25°C; rough eye phenotype at 22°C	mild rough eye phenotype 25°C; no phenotype at 22°C	mild rough eye phenotype 25°C; no phenotype at 22°C	mild rough eye phenotype 25°C; no phenotype at 22°C	mild rough eye phenotype ≥22°C
Expression in the developing wing									
nubbin (nub)-GAL4	ventral thoracic disc, wing disc, haltere disc	embryonic-adult	blister wing phenotype: 100% penetrant at ≥25°C, 50% penetrant at 22°C; minor gain-of-vein phenotype at 22°C; no serration at 22°C	blister wing phenotype: 100% penetrant ≥25°C, 99% penetrant at 22°C; minor gain-of-vein phenotype at 22°C; prominent serration at 22°C	lethal at 29°C; blister wing phenotype: 100% penetrant in escapers at 25°C, 98% penetrant at 22°C; moderate serration at 22°C (gain-of-vein not assessed)	blister wing phenotype: 100% penetrant at ≥25°C, 26% penetrant at 22°C; minor gain-of-vein phenotype at 22°C; no serration at 22°C	blister wing phenotype: 100% penetrant at ≥25°C, 14% penetrant at 22°C; minor gain-of-vein phenotype at 22°C; no serration at 22°C	blister wing phenotype: 70% penetrant at ≥25°C, 1% penetrant at 22°C; minor gain-of-vein phenotype at 22°C; no serration at 22°C	blister wing phenotype: 100% penetrant at ≥25°C, 65% penetrant at 22°C; moderate gain-of-vein phenotype at 22°C; rare serration at 22°C

* flies came up later – delayed development?

Figure S3: Extended *UAS-hTNPO2* data. (A) Expression of hTNPO2 cannot rescue lethality in *dTnpo* trans-heterozygote loss-of-function mutant animals. *UAS-hTNPO2* transgenes were expressed in the same spatiotemporal pattern as *dTnpo* using the *dTnpo CRIMIC (T2A-GAL4)* allele. Animals were trans-heterozygous for the hypomorph alleles, *dTnpo[Gly736Asp]* and *dTnpo CRIMIC*. Shown is data at 25°C while data obtained at 18°C and 22°C were consistent with these results. (**B)** The HA-tag in *hTNPO2:WT* does not significantly alter its function based on toxicity expected by calculating Mendelian ratios. 1-way ANOVA with Tukey's multiple comparisons test. P-values: **<0.01, ***<0.001. Error bars denote SD. Each dot represents one independent cross with >100 animals scored. The mean from three independent crosses is shown. **(C)** Table summarizing the impacts of ectopically expressing *UAS-hTNPO2* lines in different fly tissues and at different temperatures under control of the *GAL4/UAS* system. Red and orange indicate more severe phenotypes occur when compared to $hTNPO2{:}WT^{HA}$, with red highlighting when stronger impacts are observed. Green indicates a less severe phenotype occurs when compared to $hTNPO2{:}WT^{HA}$. Black indicates phenotypes that are similar to $hTNPO2{:}WT^{HA}$.

Fly Line	Genotype	Source
dTnpo RNAi-2 (used in [6])	*w*;; P{KK108990}VIE-260B*	VDRC #105181
dTnpo RNAi-1	*y[1] v[1]; P{TRiP.HMJ23009}attP40;*	BDSC #61230
Control (Luciferase) RNAi	*y[1] v[1];; P{y[+t7.7] v[+t1.8]=TRiP.JF01355}attP2*	BDSC #31603
Control (EGFP) RNAi	*y[1] sc[*] v[1] sev[21]; P{y[+t7.7] v[+t1.8]=VALIUM22-EGFP.shRNA.1}attP40*	BDSC #41557
ey-GAL4 (on II)	*w[*]; P{w[+m*]=GAL4-ey.H}3-8;*	BDSC #5534
GMR-GAL4 (on II)	*w[*]; P{w[+mC]=GAL4-ninaE.GMR}12;*	BDSC #1104
da-GAL4 (on III)	*w[*];; P{w[+mW.hs]=GAL4-da.G32}UH1, Sb[1]*	BDSC #55851
nub-GAL4 (on II)	*w[*]; P{w[nub.PK]=nub-GAL4.K}2;*	BDSC #86108
insc-GAL4 (on II)	*w[*]; P{w[+mW.hs]=GawB}insc[Mz1407]*	BDSC #8751
elav-GAL4^{GS} (on III)	*y[1] w[*];; P{w[+mC]=elav-Switch.O}GSG301*	BDSC #43642
ey-FLP, GMR-lacZ;; RpS17[4], w+ FRT80B	*y[d2] w[1118] P{ry[+t7.2]=ey-FLP.N}2 P{5xglBS-lacZ.38-1}TPN1;; RpS17[4] P{w[+t*] ry[+t*]=white-un1}70C P{ry[+t7.2]=neoFRT}80B/TM6B, P{y[+t7.7] ry[+t7.2]=Car20y}TPN1, Tb[1]*	BDSC #5621
Ubx-FLP	*y[1] w[*] P{w[+mC]=Ubx-FLP}1;;*	BDSC #42718
Ubi-GFP FRT80B	*w[*];; P{w[+mC]=Ubi-GFP.D}61EF P{ry[+t7.2]=neoFRT}80B*	BDSC #1620
UAS-mCherry.NLS (on III)	*w[*];; P{w[+mC]=UAS-mCherry.NLS}3*	BDSC #38424
UAS-mCD8::RFP (on II)	*w[*]; P{y[+t7.7] w[+mC]=10XUAS-IVS-mCD8::RFP}attP40;*	BDSC #32219
Df(3L)Exel8101	*w[1118];; Df(3L)Exel8101/TM6B, Tb[1]*	BDSC #7928
UAS::dTnpo^{GS11030}	*y[1] w[67c23];; P{GSV6}Tnpo[GS11030]/TM3, Sb[1] Ser[1]*	Kyoto #205260

Table S1: Publically available fly lines used in this study.

Assay	Name	Species	Forward primer (5'-3')	Reverse primer (5'-3')
Q5 mutagenesis	*TNPO2:stop*	Hsap.	tagGACCCAGCTTTCTTGTACAAAG	GACCCCATAGAAAGCCGC
	TNPO2:p.Gln28Arg	Hsap	ACAGCCACTCgGCGCATCGTG	GTTGGGCGACTGTGAGTCTTTG
	TNPO2:p.Asp156Asn	Hsap	GATCTGTGAAaACTCATCAGAGC	TTCTGCAGGGCTCCAAAG
	TNPO2:p.Trp370Cys	Hsap	TCTGTCCGACcGGAATTTGAG	GCATCATCATCATCGTCATC
	TNPO2:p.Trp370Arg	Hsap	TGTCCGACTGcAATTTGAGGAAG	GAGCATCATCATCATCGTC
	TNPO2:p.Ala546Val	Hsap	GGCACCCTGGtCGACTCTGTA	AATGGCGTCATAGAGGATGAGC
	TNPO2:p.Trp727Cys	Hsap	ACGCCACCTGtGCCATTGGTG	TGTTGCAGACGGAGATGAAC
Sequencing	*TNPO2* cDNA primer 1	Hsap	CACTGCAGTCCCAAGATCC	n/a
	TNPO2 cDNA primer 2	Hsap	TCCTCGCCAATGTCTTCC	n/a
	TNPO2 cDNA primer 3	Hsap	CCTGCTGGAGTGTCTGTCAT	n/a
qPCR	*Tnpo* (1:10)	Dmel.	GCCCGAATTTGTACGACAGT	GCAGATCCTCTGGTGGGTTA
	RP49 (1:100)	Dmel.	TGTCCTTCCAGCTTCAAGATGACCATC	CTTGGGCTTGCGCATTTGTG
	RPS20 (1:100)	Dmel.	CCGCATCACCCTGACATCC	TGGTGATGCGAAGGGTCTTG
	Tubulin (1:20)	Dmel.	CATCCAAGCTGGTCAGTG	GCCATGCTCATCGAGAT

Table S2: Primers used in this study.

REFERENCES

1. Coe, B.P., Witherspoon, K., Rosenfeld, J.A., van Bon, B.W.M., Vulto-van Silfhout, A.T., Bosco, P., Friend, K.L., Baker, C., Buono, S., Vissers, L.E.L.M., et al. (2014). Refining analyses of copy number variation identifies specific genes associated with developmental delay. Nature Genetics *46*, 1063–1071.

2. Lehman, A.M., McFadden, D., Pugash, D., Sangha, K., Gibson, W.T., and Patel, M.S. (2008). Schinzel-Giedion syndrome: report of splenopancreatic fusion and proposed diagnostic criteria. Am J Med Genet A *146A*, 1299–1306.

3. Barington, M., Risom, L., Ek, J., Uldall, P., and Ostergaard, E. (2018). A recurrent de novo CUX2 missense variant associated with intellectual disability, seizures, and autism spectrum disorder. European Journal of Human Genetics *26*, 1388–1391.

4. Lindstrand, A., Grigelioniene, G., Nilsson, D., Pettersson, M., Hofmeister, W., Anderlid, B.-M., Kant, S.G., Ruivenkamp, C.A.L., Gustavsson, P., Valta, H., et al. (2014). Different mutations in PDE4D associated with developmental disorders with mirror phenotypes. J Med Genet *51*, 45–54.

5. Link, N., Chung, H., Jolly, A., Withers, M., Tepe, B., Arenkiel, B.R., Shah, P.S., Krogan, N.J., Aydin, H., Geckinli, B.B., et al. (2019). Mutations in ANKLE2, a ZIKA Virus Target, Disrupt an Asymmetric Cell Division Pathway in Drosophila Neuroblasts to Cause Microcephaly. Developmental Cell *51*, 713-729.e6.

6. Shi, Q., Han, Y., and Jiang, J. (2014). Suppressor of fused impedes Ci/Gli nuclear import by opposing Trn/Kapβ2 in Hedgehog signaling. J Cell Sci *127*, 1092–1103.